Journal of Global Positioning Systems (2024)
Vol. 20, Joint No. 1 & No. 2: 1-12
DOI:10.5081/jgps.20.1.1

Refinement of elevation angle based stochastic model and positioning performance for QZSS

Yao Zong[1], Kaifei He[1,2]✉, Xuchen Ma[1], Kai Ding[3], Yu Fu[1], Xiang Xu[1]

1. College of Oceanography and Space Informatics, China University of Petroleum (East China), Qingdao 266580, China
2. Technology Innovation Center for Maritime Silk Road Marine Resources and Environment Networked Observation, Ministry of Natural Resources, Qingdao 266580, China
3. Shandong Vocational College of Information Technology, Weifang 261061, China

✉ Corresponding author, kfhe@upc.edu.cn

Abstract: An improved stochastic model refinement method is proposed to address the discrepancies in observation quality between the Quasi-Zenith Satellite System (QZSS) and the Global Positioning System (GPS). The proposed method refines the traditional empirical stochastic model of elevation angle to enhance the accuracy of baseline solutions. Specifically, the parameters of the refined model are estimated based on the least squares method by counting the time series of single difference residuals of QZSS/GPS satellites and analyzing their relationship with the change of elevation angle. To evaluate its effectiveness, the positioning accuracy of the refined model is comparatively assessed against that of the empirical model through baseline experiments of varying lengths. The results indicate that GPS satellite observations exhibit higher accuracy than those of QZSS. Moreover, compared with the empirical model, the refined model significantly improves positioning accuracy and stability. In the East, North, and Up, the root mean square (RMS) errors are reduced by at least 25.01%, 42.08%, and 4.37%, respectively, yielding an overall average positioning accuracy improvement of more than 31.92%.

Key words: QZSS; GPS; Single difference residual; stochastic model

1. Introduction

The function model describes the interrelationships among observations, as well as between observations and unknown parameters, while the stochastic model characterizes the random properties of observation errors. The accuracy of both models directly influences the precision and reliability of multi-system positioning, making it essential to analyze the accuracy and stochastic statistical properties of satellite observations across different systems and frequencies[1]. The establishment and refinement of the stochastic model is a crucial component of high-precision positioning, as it has a significant impact on the final positioning accuracy[2-3]. Currently, three main types of stochastic models are commonly used: the satellite elevation angle model, the signal-to-noise ratio (SNR) model, and the posterior variance component estimation model. Zhang[4] analyzed the observation quality of BeiDou II and developed a stochastic model suitable for BeiDou solutions based on a refined elevation angle weighted model and an SNR-weighted model

Editor-In-Charge: Dr. Wu Chen

using zero-baseline single difference residuals. Cai[5] refined a hybrid stochastic model combining elevation angle and SNR by extracting pseudorange and carrier phase noise from GPS, BDS, and Galileo observations through inter-station single difference and inter-epoch triple-difference. Wu[6] applied the least squares variance component estimation method to estimate the variance of BeiDou single difference observations and proposed a stochastic modeling strategy for relative positioning. Dai[7] evaluated stochastic models based on satellite elevation angle, carrier-to-noise ratio, and signal strength using real observation data, and demonstrated that the models based on signal strength and carrier-to-noise ratio perform similarly and are effective in mitigating atmospheric delays, multipath, and other errors, while the elevation angle model is particularly effective in reducing residual tropospheric delay errors. Prochniewicz[8] conducted a detailed investigation of stochastic modeling methods for multi-GNSS systems including GPS, GLONASS, Galileo, and BDS. Li[9] collected ultra-short baseline GPS observations at a 1-second sampling interval with different receiver types, and examined the variance, observation accuracy, and correlations of the stochastic model, including elevation angle correlation, temporal correlation, and inter-type correlations.

Moreover, with the development of regional satellite navigation systems, increasing attention has been directed toward refining positioning performance and observation models. The proper construction of a stochastic model for QZSS is particularly significant for enhancing the accuracy and reliability of augmented information products. Pu[10] presented a comprehensive review of the current status and development trends of Japan's regional navigation satellite system, with a focus on the high-precision augmentation services provided by QZSS, which also offer valuable insights for improving other global and regional navigation systems. Li[11] evaluated the performance of precise point positioning (PPP) using only the four QZSS satellites in both static and kinematic scenarios, demonstrating the preliminary capability of QZSS for independent navigation and positioning. Kawate[12] improved positioning accuracy by refining observation models and processing algorithms based on QZSS augmentation products. Bramanto[13] investigated the static PPP performance with QZSS augmentation information, using high-precision relative positioning results as a benchmark. Collectively, these studies provide a solid foundation for further exploration of QZSS positioning capabilities and the optimization of its associated observation models.

In summary, research on the accuracy of observations and stochastic modeling for systems such as GPS, BDS, and Galileo has reached a relatively mature stage both domestically and internationally, whereas studies focusing on QZSS remain limited. To address this gap, this paper employs zero- and short-baseline single difference residual methods to evaluate and analyze the accuracy of pseudorange and carrier phase observations from QZSS and GPS satellites. By examining the relationship between elevation angle and observation accuracy, the least squares method is applied to estimate the parameters of the elevation angle stochastic model for QZSS and GPS. Based on the fitted parameters, a combined stochastic model for QZSS and GPS positioning is constructed, providing a theoretical basis for the rational development of integrated stochastic models in GNSS positioning.

2. Zero/short-baseline inter-station single difference residual model

By connecting two or more receivers to the same antenna through a power divider to form a zero-baseline[14], most of the error is eliminated by the difference due to the short distance between the two receivers. Short-baseline means that the distance between two GNSS receivers is relatively short, usually no more than ten kilometers, and the tropospheric and ionospheric delays are similar between the two receivers, and most of the errors can likewise be eliminated by difference. The inter-station single difference model preserves the

error characteristics of a single satellite by differencing observations from two different stations, for the same satellite, and is suitable for evaluating the data quality and error characteristics of a single satellite. The original observation equations of two stations observing the same satellite at the same epoch are differenced to obtain the single difference observation equations between the stations, and the single difference observation equations for the carrier observations, for example, are as follows[15]:

$$\lambda\Delta\varphi_{ur}^{s} = \Delta r_{ur}^{s} + c\Delta t_{ur} + \Delta T_{ur}^{s} - \Delta I_{ur}^{s} + \lambda N_{ur}^{s} + \Delta\delta_{ur} + \Delta\varepsilon_{ur}^{s} \quad (1)$$

where Δ is the single difference operator, s is the observation satellite number; u and r is two different receivers; λ denotes the wavelength; r_{ur}^{s} denotes the geometrical distance from the receiver to the satellite; c is the speed of light in a vacuum; t_{ur} is the receiver clock error; T_{ur}^{s} stands for the tropospheric delay; I_{ur}^{s} stands for the ionospheric delay; N_{ur}^{s} denotes the single difference ambiguity; $\Delta\delta_{ur}$ denotes the phase delay at the receiver; and ε_{ur}^{s} stands for the measurement noise.

Based on the above analysis and Eq. (1), the single difference observation equation for the short-baseline case is derived as:

$$\lambda\Delta\varphi_{ur}^{s} = \Delta r_{ur}^{s} + c\Delta t_{ur} + \lambda N_{ur}^{s} + \Delta\delta_{ur} + \Delta\varepsilon_{ur}^{s} \quad (2)$$

It should be noted that the effects of tropospheric delay T_{ur}^{s} and ionospheric delay I_{ur}^{s} on the baseline solution become progressively more pronounced as the baseline length increases, and therefore the effects of other factors on the various types of observations need to be evaluated. Since this study only deals with zero- and short-baseline data, the single difference residual model between stations for the long baseline case will not be elaborated in detail.

3. Refinement of QZSS/GPS stochastic model based on single difference residuals

A stochastic model based on elevation angle is a function used to characterize the noise level of observations, using the elevation angle of the satellite as a measure. In general, as the satellite elevation angle increases, the quality of observation data is less affected by multipath and atmospheric errors. The more widely used elevation angle functions are trigonometric functions, segmented functions, etc., such as the sine function model used by GAMIT. The aim of this paper is to develop a stochastic model of QZSS and GPS observations with respect to the elevation angle and implement it based on the TrackRT[16] software. Taking the elevation angle as the independent variable, the functional expression of the sinusoidal elevation angle stochastic model is:

$$\sigma^{2} = m^{2} + \frac{n^{2}}{\sin^{2}(elev)} \quad (3)$$

where $elev$ is the satellite elevation angle; σ is the error in the observation; m, n are empirical coefficients.

The single difference residuals of pseudorange and carrier phase observations of QZSS and GPS satellites are calculated according to Eqs. (1) and (2), and in this way, a stochastic model of observations conforming to QZSS/GPS is established. In order to better analyze the pseudorange and carrier phase single difference residual values of QZSS and GPS satellites, and to take into account the influence of the satellite elevation angle, the following calculation scheme is adopted[1]: Group elevation angles in units of 1°, e.g., for intervals of $20.5° \leq elev < 21.5°$, calculate the standard deviation of the single difference residuals for all satellites in the interval, and use this value as the corresponding single difference residual value for an elevation angle of 21°. The specific method is as follows: based on the single difference residual time series obtained from the previous calculations, all satellites under each elevation angle are analyzed, and their single difference residual standard deviations are calculated; based on the relationship between the standard deviation and the elevation angle and combining with Eq. (3), the observation equation (4) is constructed, and the coefficient matrix A and the observation value matrix L are obtained from the observation equation; and the stochastic model coefficients m, n are calculated based on the least squares.

The observation equation constructed through the above steps is shown below:

$$\begin{bmatrix} \hat{\sigma}_1^2 \\ \hat{\sigma}_2^2 \\ \vdots \\ \hat{\sigma}_j^2 \end{bmatrix} = \begin{bmatrix} 1 & \frac{1}{\sin^2(elev_1)} \\ 1 & \frac{1}{\sin^2(elev_2)} \\ \vdots & \vdots \\ 1 & \frac{1}{\sin^2(elev_j)} \end{bmatrix} \begin{bmatrix} m^2 \\ n^2 \end{bmatrix} \quad (4)$$

where

$$A = \begin{bmatrix} 1 & \frac{1}{\sin^2(elev_1)} \\ 1 & \frac{1}{\sin^2(elev_2)} \\ \vdots & \vdots \\ 1 & \frac{1}{\sin^2(elev_j)} \end{bmatrix},$$

$$L = \begin{bmatrix} \hat{\sigma}_1^2 & \hat{\sigma}_2^2 & \cdots & \hat{\sigma}_j^2 \end{bmatrix}^T \quad X = \begin{bmatrix} m^2 & n^2 \end{bmatrix}^T \quad (5)$$

where j is the number of satellites; the parameters to be solved are m, n. According to the principle of least squares, the model coefficients can be solved:

$$X = (A^T PA)^{-1} A^T PL \quad (6)$$

where P is the observation weight matrix, A is the coefficient matrix, and L is the observation matrix. After refining the stochastic model, each type of observation corresponds to a set of m, n values.

4. QZSS/GPS data collection and result analysis

4.1 QZSS/GPS pseudorange and carrier phase measurement accuracy

Two stations at Curtin University, Australia, namely CUT0 and CUT2, were selected to form a zero-baseline. Additionally, two short baselines were formed by the station pairs CUT2-CUTB and CUT0-CUTC. Observation data from all six stations were continuously collected over a 10-day period, from January 4 to January 13, 2023 (DOY 004-013), with a sampling interval of 30 s. Table 1 summarizes the details of each station at Curtin University.

Based on the zero- and short-baseline single difference solution models, the single difference residual values of the pseudorange and carrier phase observations of QZSS and GPS satellites were calculated. In order to study its characteristics in detail, Figure 1 shows the single difference residual time series of pseudorange and carrier phase observations of GPS satellites at zero-baseline, and in this paper, one satellite from each of the three different types of GPS satellites is selected as a representative, i.e., GPS IIF (G08), GPS III (G18) and GPS IIR (G29), and from this, we obtain the accuracy of the pseudorange and carrier phase observation values of the GPS satellite statistical results, as shown in Table 2.

From Figure 1 and Table 2, it can be concluded that the pseudorange single difference residuals of GPS satellites basically fluctuate within the interval of -1~1 m, and the accuracy of the pseudorange observation values of GPS P1 is about 20 cm, and the accuracy of the pseudorange observation values of P2 is about 24 cm; the carrier phase single difference residuals of GPS satellites basically fluctuate within the interval of -5~5 mm, and the accuracy of the carrier phase observations values of GPS L1, L2 are all in the range of 1 mm. It also verifies the conclusion that the accuracy of the carrier phase observations is significantly higher than that of the pseudorange observations.

Figure 2 illustrates the pseudorange and carrier phase observations single difference residual time series of two different orbit types of QZSS satellites, namely QZSS QZO (J02, J03, J04) and QZSS GEO (J07), for short-baseline. From Figure 2 and Table 2, it can be concluded that the pseudorange single difference residuals of QZSS satellite basically fluctuate in the range of -2~2 m, and the accuracy of QZSS P1 pseudorange observation value is about 58 cm, and the accuracy of P2 pseudorange observation value is about 33 cm; the carrier phase single difference residuals of QZSS satellite basically fluctuate in the range of -10 mm~10 mm, and the accuracy of L1, L2 carrier phase observation value is about 2.32 mm. In summary, it can be concluded that

in the case of zero- or short-baseline, the accuracy of the observed values of GPS satellites is better than that of QZSS satellites as a whole.

Tab.1 Information of the measuring station

Stations		Antenna type	Receiver types	Sample interval (s)
	CUT0		TRIMBLE NETR9	30
CUT00	CUT2	TRM 59800.00 SCIS	TRIMBLE NETR9	30
	CUT3		JAVAD TRE_G3TH_8	30
	CUTA		TRIMBLE NETR9	30
CUTA0	CUAA	TRM 59800.00 SCIS	JAVAD TRE_G3TH_8	30
	CUAI		SEPTENTRIO POLARXS	30
	CUBB		JAVAD TRE_G3TH_8	30
CUTB0	CUTB	TRM 59800.00 SCIS	TRIMBLE NETR9	30
	CUBJ		JAVAD TRE_G3TH_DELTA	30
	CUCC		JAVAD TRE_G3TH_8	30
CUTC0	CUTC	TRM 59800.00 SCIS	TRIMBLE NETR9	30
	CUBS		SEPTENTRIO POLARX5	30

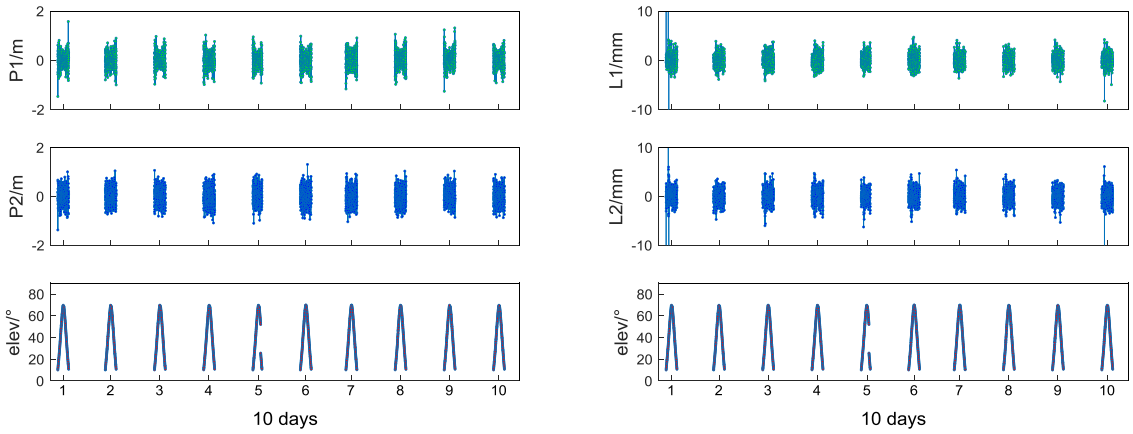

(a) G08 (left : pseudorange; right : carrier phase)

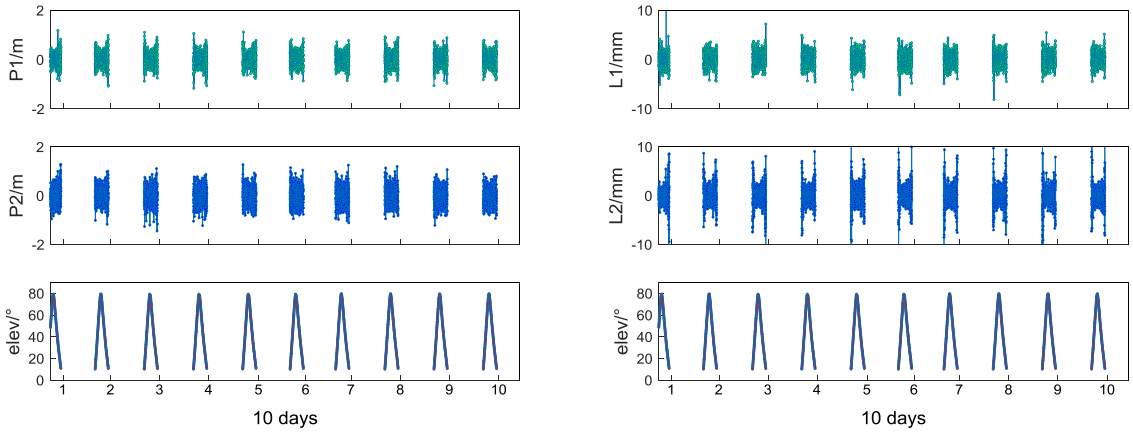

(b) G18 (left : pseudorange; right : carrier phase)

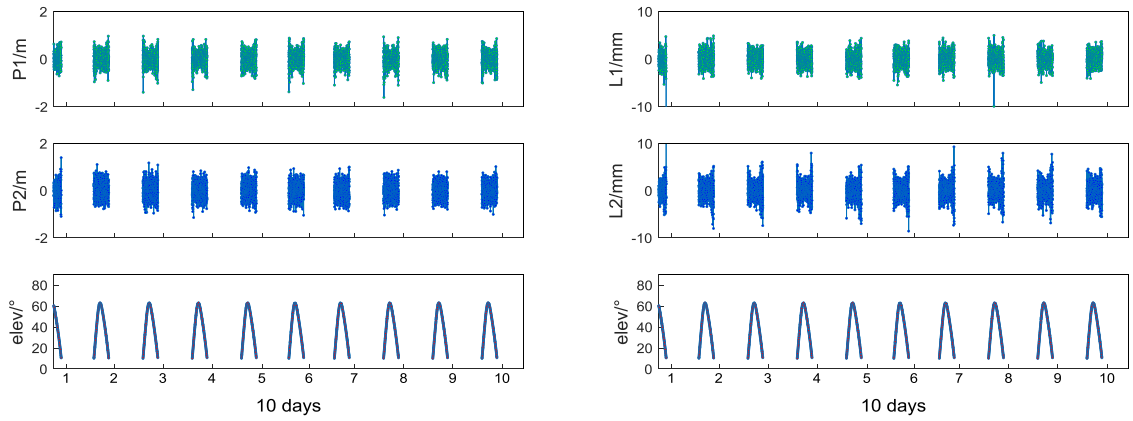

(c) G29 (left : pseudorange; right : carrier phase)

Fig.1 Time series of zero-baseline residuals for GPS pseudorange and carrier phase

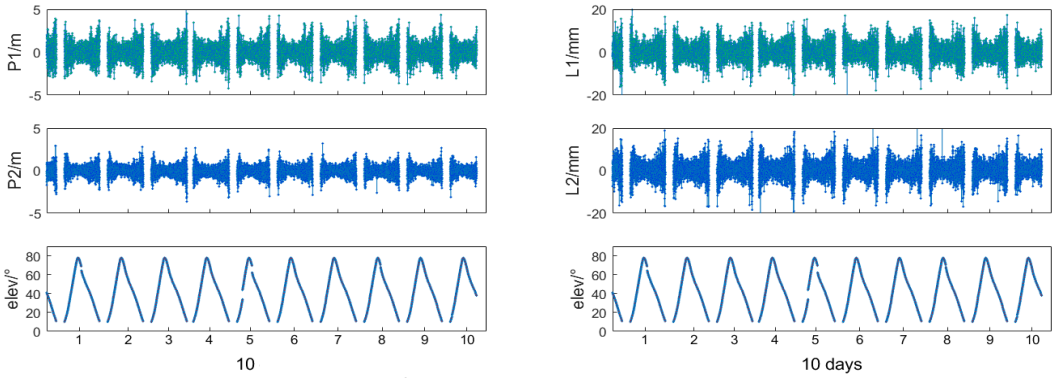

(b) J02 (left : pseudorange; right : carrier

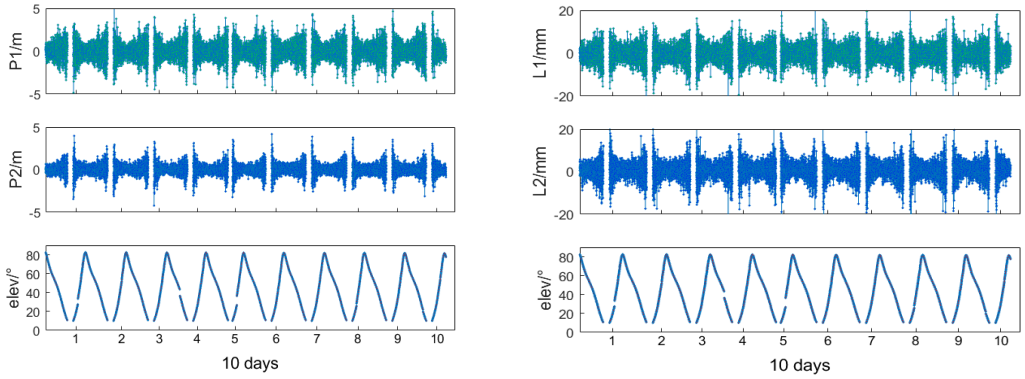

(b) J03 (left : pseudorange; right : carrier phase)

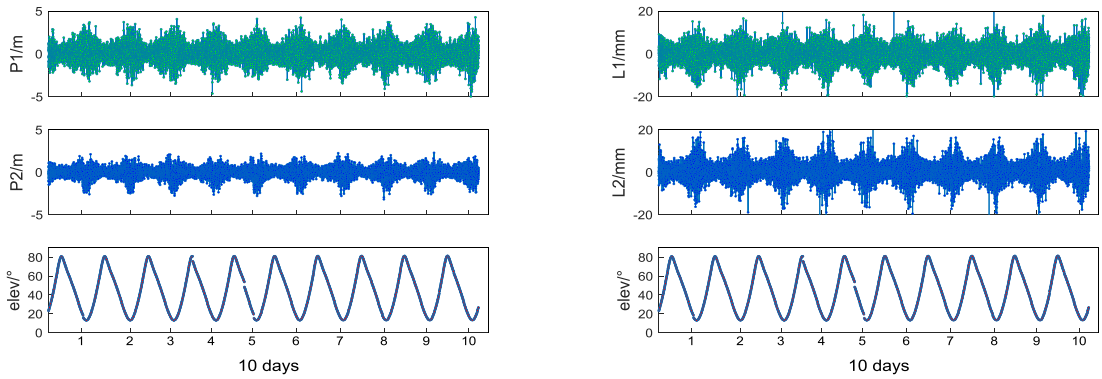

(c) J04 (left : pseudorange; right : carrier phase)

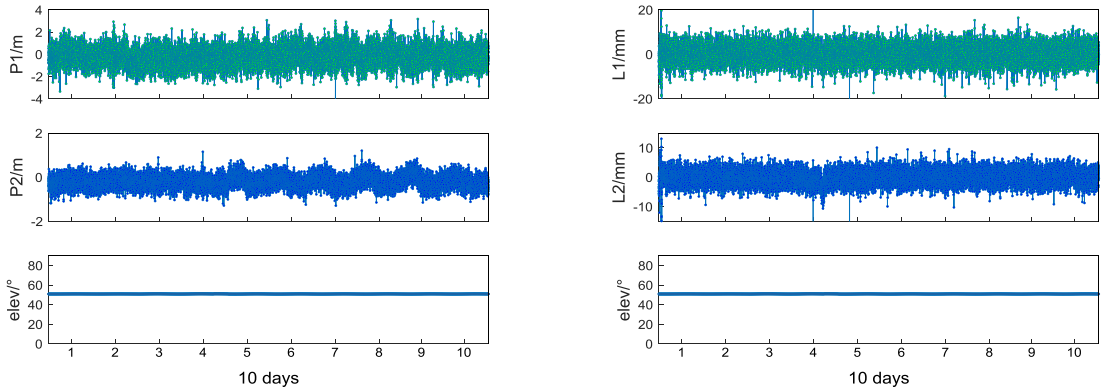

(d) J07 (left : pseudorange; right : carrier phase)

Fig.2 Time series of short-baseline residuals for QZSS pseudorange and carrier phase

Tab.2 GPS/QZSS pseudorange and carrier phase observations accuracy

Satellite systems	Orbit types	PRN	Pseudorange observation/m		Carrier phase observation/mm	
			P1	P2	L1	L2
GPS	MEO	G08	0.194	0.235	0.816	0.942
	MEO	G18	0.187	0.242	0.895	1.230
	MEO	G29	0.187	0.231	0.925	1.162
QZSS	QZO	J02	0.518	0.314	2.086	2.104
	QZO	J03	0.551	0.331	2.212	2.275
	QZO	J04	0.656	0.406	2.731	2.762
	GEO	J07	0.600	0.273	2.681	1.728

4.2 Determination of QZSS/GPS stochastic model coefficients

Figures 3~4 illustrate the standard deviation of carrier phase residuals with respect to the satellite elevation angle for QZSS and GPS (satellite cut-off angle set to 10°). Overall, the results indicate that the standard deviation of carrier phase residuals increases as the satellite elevation angle decreases. Based on the least squares principle, the elevation angle model coefficients for pseudorange and carrier phase observations of QZSS and GPS satellites across different orbit types and frequencies were estimated. The detailed fitting results are summarized in Table 3.

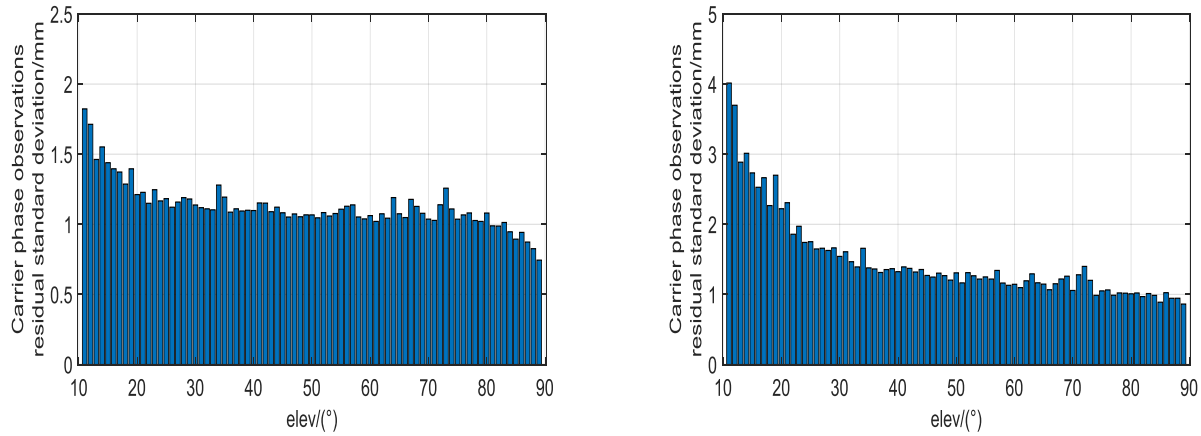

Fig.3 Relation between carrier phase observations residual standard deviation and elevation angle of GPS satellite (left : GPS L1; right : GPS L2)

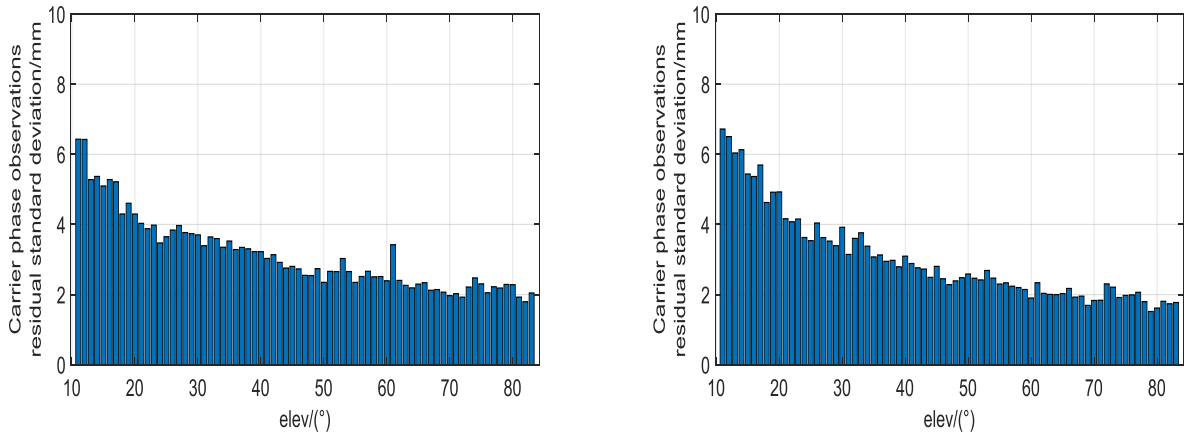

Fig.4 Relation between carrier phase observations residual standard deviation and elevation angle of QZSS satellite (left : QZSS L1; right : QZSS L2)

Tab.3 The fitted values of QZSS/GPS pseudorange and carrier phase observations

Observation types	Model coefficients	MEO (GPS)		IGSO (QZSS)	
		L1	L2	L1	L2
Pseudorange	*m*	0.174	0.265	0.536	0.206
	n	0.079	0.063	0.301	0.220
Carrier phase	*m*	1.005	0.767	2.193	1.786
	n	0.276	0.715	1.216	1.344

From Figures 3~4 and Table 3, the fitted stochastic model coefficients of QZSS IGSO satellites at the L1 frequency are m = 0.536 and n = 0.301 for pseudorange observations, and m = 2.193 and n = 1.216 for carrier phase observations. At the L2 frequency, the coefficients are m = 0.206 and n = 0.220 for pseudorange, and m = 1.786 and n = 1.344 for carrier phase. For GPS MEO satellites, the coefficients at the L1 frequency are m = 0.174 and n = 0.079 for pseudorange, and m = 1.005 and n = 0.276 for carrier phase; at the L2 frequency, they are m = 0.265 and n = 0.063 for pseudorange, and m = 0.767 and n = 0.715 for carrier phase.

Figure 5 presents the fitted stochastic model curves for the QZSS/GPS satellite carrier phase observations. To better illustrate the statistical characteristics, a 95% confidence interval (CI) is shown as light-shaded areas, representing the possible variation range of the residual standard deviation with respect to satellite elevation angle at the given confidence level.

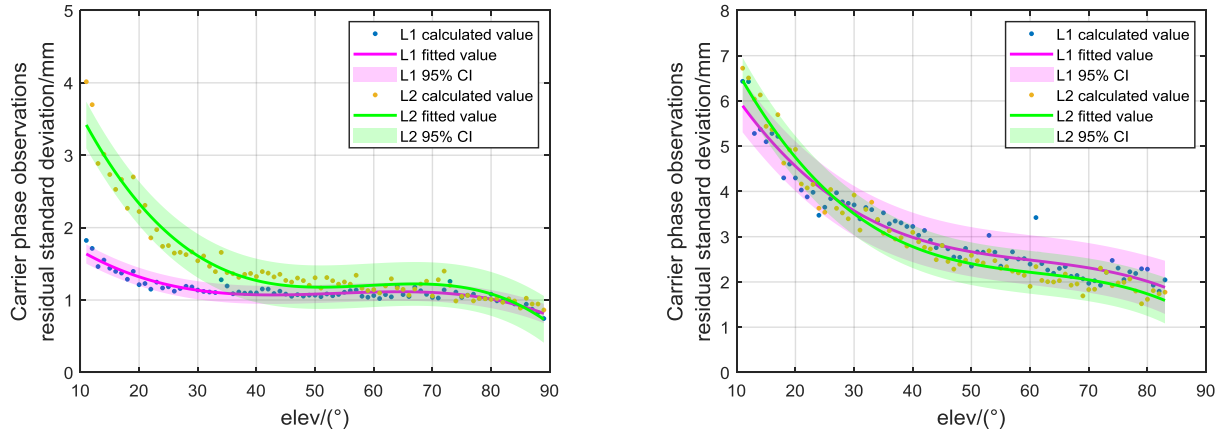

Fig.5 Carrier fitting curves of stochastic model (left : GPS; right : QZSS)

4.3 Analysis of the positioning accuracy

To evaluate the positioning performance of the refined stochastic model, two baselines of different lengths were selected for the combined QZSS/GPS positioning test: STR1-TID1 in eastern Australia and ISHI-TSK2 in central Japan. The processing strategies are summarized in Table 4. Both the empirical and refined models were applied to perform real-time relative positioning on the two baselines, with a satellite elevation cutoff angle of 10°. The static positioning results were then compared against the known reference coordinates [17]. In this study, the precise coordinates provided by the IGS were adopted as the ground truth for calculating positioning errors.

The positioning errors of STR1-TID1 under the two stochastic models in the E, N, and U directions are shown in Figure 6. It can be observed that the error variations in each direction are smoother when using the refined stochastic model. The positioning errors of ISHI-TSK2 under the two models are shown in Figure 7. With the longer baseline, positioning errors increase in all directions; moreover, while the empirical model exhibits occasional large fluctuations in the error time series, the refined model shows significantly smaller amplitudes and smoother variations. Across both baseline experiments, the refined model also demonstrates a notably faster convergence time compared to the empirical model.

To further evaluate the optimization effect of the refined model, Table 5 presents the statistical analysis of RMS values and point accuracy for two baselines under both the refined and empirical stochastic models in the E, N, and U directions. The results clearly demonstrate that the refined model improves positioning accuracy for both baselines, though to varying degrees. For the STR1-TID1 baseline, improvements of over 40% were observed in the E, N, and U directions, with an overall point accuracy improvement of 50.87%. For the ISHI-TSK2 baseline, the greatest enhancement was in the N direction with 84.20%, while the E and U directions improved by 25.01% and 4.37%, respectively, yielding an overall point accuracy improvement of 31.92%. Compared with STR1-TID1, the accuracy of ISHI-TSK2 decreased, which can be attributed to the longer baseline length. Furthermore, the Wilcoxon signed-rank test[18] was applied to assess the statistical significance of positioning errors in the E, N, and U directions before and after refinement. The results confirm that improvements in all three directions are statistically significant, indicating that the refined model has a substantial effect on positioning accuracy. Overall, the refined stochastic model enhances the accuracy of real-time relative positioning and demonstrates greater stability than the empirical model. Nevertheless, further experiments are recommended to comprehensively validate the robustness of the refined model.

5 Conclusions

In this paper, we address the problem of differences in the quality of QZSS/GPS satellite observations and refine the traditional empirical elevation angle stochastic model to improve baseline solution accuracy. Using the single difference residuals from zero- and short-baseline stations, we refine the stochastic model of QZSS/GPS observations by analyzing the time series of residuals and their relationship with satellite elevation angle. The parameters of the refined model are then estimated with the least squares method. Furthermore, real-time relative positioning experiments with different baseline lengths are conducted to compare and analyze the positioning accuracy of the refined model against that of the empirical model. In addition, the high-precision augmentation services provided by QZSS present new opportunities for the advancement of navigation and positioning technology. This also points to the direction of future research. In the coming years, QZSS is expected to be expanded into a constellation of seven satellites[19], which will enable broader coverage and higher positioning accuracy.

Acknowledgments

This work is supported by the National Natural Science Foundation of China (42574034, 42174021), the Fundamental Research Funds for the Central Universities (24CX02031A) and the Shandong Provincial Natural Science Foundation, China (ZR2021MD060). Thanks the Curtin GNSS-SPAN Group in Australia, the International GNSS Service (IGS), the Multi-GNSS Integrated Real-time and Archived Information system (MIRAI) in Japan for providing real-time GNSS observations.

Tab.4 Processing strategies

Parameters	Processing Method
Observations	Carrier phase / pseudorange observations
Systems	GPS/QZSS
Elevation Cut-off Angle	10°
Sampling Interval	1s
Baseline Mode	Short
Code Bias	DCB
Phase Center Offset	Model correction
Receiver Clock Error	Estimated
Phase Ambiguity	MW-WL ambiguity resolution
Tropospheric Delay	GPT model correction
Atmospheric Delay	GMF model correction
Global Tidal Model	OTL FES 2004

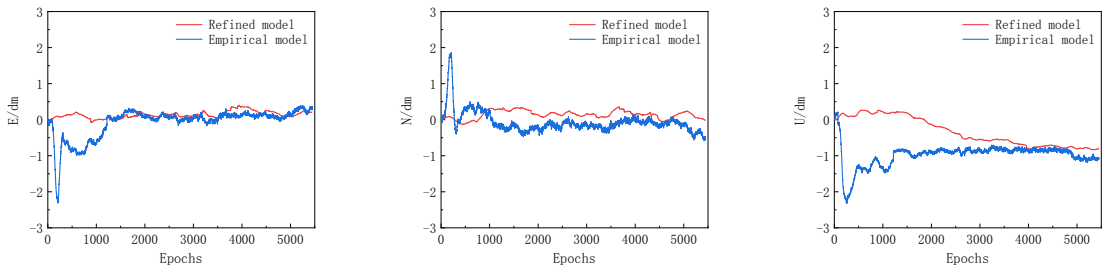

Fig.6 STR1-TID1 different stochastic model error plot in each direction

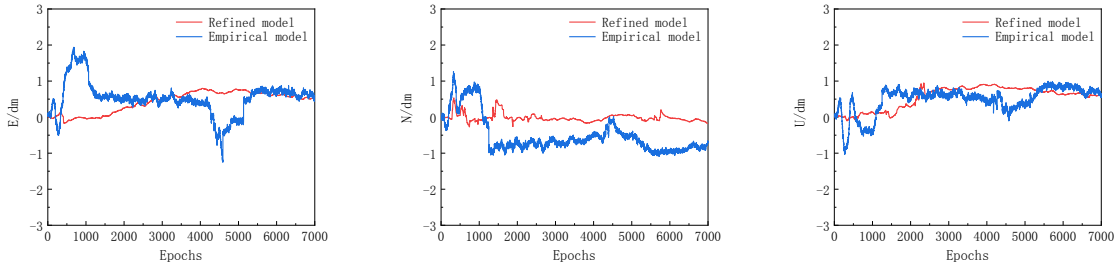

Fig.7 STR1-TID1 different stochastic model error plot in each direction

Tab.5 RMS values and point accuracy statistics of different baselines in each direction

Baselines	Baseline length/km	Stochastic model	RMS/mm			Point accuracy/mm
			E	N	U	
STR1-TID1	9.7	Empirical model	42.65	31.18	103.70	116.38
		Refined model	16.65	18.06	51.64	57.18
		Improvement rate	60.69%	42.08%	50.20%	50.87%
ISHI-TSK2	16.5	Empirical model	68.82	72.09	63.37	118.11
		Refined model	51.61	11.39	60.60	80.41
		Improvement rate	25.01%	84.20%	4.37%	31.92%

References

[1] LIU Y J, JIANG Y. Precision Analysis of the BDS GEO/IGSO/MEO Observables and Stochastic Model Refining [J]. GNSS World China, 2018, 43(01): 1-6.

[2] HU H, XIE X F, GAO J X, et al. GPS-BDS-Galileo double-differenced stochastic model refinement based on least-squares variance component estimation [J]. Journal of Navigation, 2021: 1-16.

[3] ZENG Q. Research on Method and Quality Control for BDS/GPS Combined Kinematic Relative Positioning [D]. Wuhan: Wuhan University, 2018.

[4] Zhang X H, DING L L. Quality Analysis of the Second Generation Compass Observables and Stochastic Model Refining [J]. Geomatics and Information Science of Wuhan University, 2013, 38(07): 832-836.

[5] CAI Q Q, ZHU F, CHEN X, et al. Refinement of GNSS stochastic model combining elevation angle and SNR and its effect on RTK positioning performance [J]. GNSS World of China, 2023, 48(1): 24-31.

[6] WU S S, ZHAO X B, PANG C L, et al. Stochastic modeling strategy for BDS hybrid constellation in relative positioning [J]. Journal of National University of Defense Technology, 2019, 41(05): 43-48.

[7] DAI W J, DING X L, ZHU J J. Comparing GPS Stochastic Models Based on Observation Quality Indices [J]. Geomatics and Information Science of Wuhan University, 2008, (07): 718-722.

[8] PROCHNIEWICZ D, WEZKA K, KOZUCHOWSKA J. Empirical Stochastic Model of Multi-GNSS Measurements [J]. Sensors, 2021, 21(13): 4566.

[9] LI B F, SHEN Y Z, XU P L. Assessment of stochastic models for GPS measurements with different types of receivers [J]. Chinese Science Bulletin, 2008, 53(20): 3219-3225.

[10] PU G Y. The developed procedures and developing trends of the Japanese navigation satellites [J]. Journal of Navigation and Positioning, 2022, 10(2): 21-25.

[11] LI X P, PAN L, YU W K. Assessment and Analysis of the Four-Satellite QZSS Precise Point Positioning and the Integrated Data Processing With GPS [J]. IEEE Access, 2021, 9: 116376-116394.

[12] KAWATE K, IGARASHI Y, YAMADA H, et al. MADOCA: Japanese precise orbit and clock determination tool for GNSS [J]. Advances in Space Research, 2023, 71(10): 3927-3950.

[13] BRAMANTO B, THERESIA R, GUMILAR I, et al. Performance of GNSS positioning in PPP mode using MADOCA precise products [J]. Geodesy and Geodynamics, 2024, 15(6): 642-651.

[14] YANG Y X, LI J L. WANG A B, et al. Preliminary assessment of the navigation and positioning performance of BeiDou regional navigation satellite system [J]. Science China: Earth Sciences, 2014, 44(01): 72-81.

[15] LIU L. Research on Method of GNSS Observation Precision Estimation and Stochastic Model Refinement [D]. Wuhan: Wuhan University, 2019.

[16] NIU B. High-rate GPS real-time kinematic positioning research [D]. Wuhan: Institute of Seismology, China Earthquake Administration, 2013.

[17] HE K F, WANG Z J, WANG X L, et al. The Precision Evaluation and Analysis of GNSS Precise Positioning for Highly Dynamic Platform [J]. Journal of Navigation and Positioning, 2015, 3(03): 69-73+116.

[18] Wilcoxon, F. Individual Comparisons by Ranking Methods [J/OL]. Biometrics Bulletin, 1945, 1(6): 80.

[19] SAKAI T. Japanese GNSS Future System Evolution in the 2020-2030 Perspective [J]. European Navigation Conference (ENC), 2020:

1-10.

Authors

Yao Zong is a Ph.D. candidate of China University of Petroleum (East China). His research mainly focuses on GNSS relative positioning and augmentation information.

Kaifei He is a professor at the China University of Petroleum (East China). He received his Ph.D. degree in Geodesy from the Technical University of Berlin in 2015 and studied in GFZ as a Ph.D. student from 2010 to 2014. Currently, his research focuses on GNSS navigation and positioning algorithms, underwater positioning, geodesy data processing, and software development.

XuChen Ma is a graduate student of China University of Petroleum (East China). His research focused on Multi-system high-precision dynamic real-time positioning.

Kai Ding is a lecturer at Shandong Vocational College of Information Technology. He received his Master degree in Geodesy and Survey Engineering from Shandong University of Science and Technology in 2010. Currently, his research focuses on GNSS data processing and UAV mapping.

Yu Fu is a graduate student of China University of Petroleum (East China). His research focused on GNSS speed measurement.

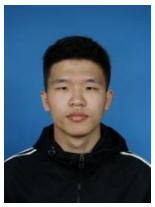

Xiang Xu is a graduate student of China University of Petroleum (East China). His research focused on GNSS/INS integrated navigation filtering algorithm.